

Machine Learning Predictions of Molecular Properties: Accurate Many-Body Potentials and Nonlocality in Chemical Space

Katja Hansen,[†] Franziska Biegler,[‡] Raghunathan Ramakrishnan,[§] Wiktor Pronobis,[‡] O. Anatole von Lilienfeld,^{§,||} Klaus-Robert Müller,^{*,‡,⊥} and Alexandre Tkatchenko^{*,†}

[†]Fritz-Haber-Institut der Max-Planck-Gesellschaft, Faradayweg 4-6, 14195, Berlin, Germany

[‡]Machine Learning Group, Technical University of Berlin, Marchstr. 23, 10587 Berlin, Germany

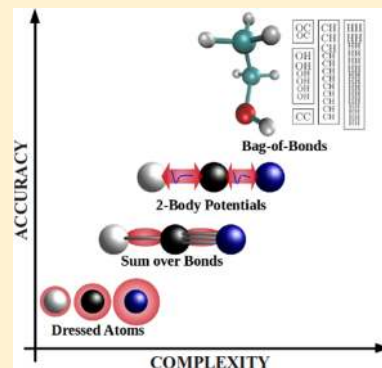
[§]Institute of Physical Chemistry and National Center for Computational Design and Discovery of Novel Materials, Department of Chemistry, University of Basel, Klingelbergstrasse 80, CH-4056 Basel, Switzerland

^{||}Argonne Leadership Computing Facility, Argonne National Laboratory, 9700 South Cass Avenue, Argonne, Illinois 60439, United States

[⊥]Department of Brain and Cognitive Engineering, Korea University, Anam-dong, Seongbuk-ku, Seoul 136-713, Korea

Supporting Information

ABSTRACT: Simultaneously accurate and efficient prediction of molecular properties throughout chemical compound space is a critical ingredient toward rational compound design in chemical and pharmaceutical industries. Aiming toward this goal, we develop and apply a systematic hierarchy of efficient empirical methods to estimate atomization and total energies of molecules. These methods range from a simple sum over atoms, to addition of bond energies, to pairwise interatomic force fields, reaching to the more sophisticated machine learning approaches that are capable of describing collective interactions between many atoms or bonds. In the case of equilibrium molecular geometries, even simple pairwise force fields demonstrate prediction accuracy comparable to benchmark energies calculated using density functional theory with hybrid exchange-correlation functionals; however, accounting for the collective many-body interactions proves to be essential for approaching the “holy grail” of chemical accuracy of 1 kcal/mol for both equilibrium and out-of-equilibrium geometries. This remarkable accuracy is achieved by a vectorized representation of molecules (so-called Bag of Bonds model) that exhibits strong nonlocality in chemical space. In addition, the same representation allows us to predict accurate electronic properties of molecules, such as their polarizability and molecular frontier orbital energies.



Chemical compound space (CCS) is the space populated by all possible energetically stable molecules varying in composition, size, and structure.¹ Chemical reactions and transformations due to external perturbations allow us to explore this astronomically large space to obtain molecules with desired properties (e.g., stability, mechanical, and electronic properties). The accurate prediction of these molecular properties in the CCS is a critical ingredient toward rational compound design in chemical and pharmaceutical industries. Therefore, one of the major challenges is to enable quantitative calculations of molecular properties in CCS at moderate computational cost (milliseconds per molecule or faster), however, currently only wave-function-based quantum-chemical calculations, which can take up to several days per molecule, consistently yield the desired “chemical accuracy” of 1 kcal/mol required for predictive in silico rational molecular design.

Leaving aside the quest for accuracy, even our understanding of the structure and properties of CCS is remarkably shallow. Furthermore, a unique mathematical definition of CCS is lacking because the mapping between molecular geometries

and molecular properties is often not unique, meaning that there can be structurally different molecules exhibiting very similar values for any given property. This complexity is reflected by the existence of hundreds of descriptors that aim to measure molecular similarity in chemoinformatics.^{2,3} In this context, one of our goals is to shed light into the structure and properties of CCS in terms of molecular atomization energies that is an essential molecular property measuring the stability of a molecule with respect to its constituent atoms. Atomization energies are accessible experimentally and are frequently used to assess the performance of electronic structure methods. The total energy of a molecule can be trivially determined from its atomization energy by simply adding free atom energies. Under certain conditions chemical reaction barriers can also be correlated to the difference between total energies of two molecules. Obviously, total energies are insufficient to predict the stability and reactivity of molecules in realistic environ-

Received: April 22, 2015

Accepted: June 4, 2015

$$\hat{E}_{\text{pp}}(\mathbf{M}) = \sum_{ij}^{\text{atom pairs}} \sum_r^{\text{r of type } ij} \Phi_{ij}(r) \quad (1)$$

where $\Phi(r)$ is an effective potential function for each type of atom pair ij (carbon–carbon C–C, carbon–nitrogen C–N, and so on). We note that different functional forms can be adopted for $\Phi(r)$, ranging from Lennard-Jones and Morse-type to more general polynomial potentials. Already the usage of Lennard-Jones potential yields an accuracy of 8.7 kcal/mol on the GDB-7 database. This is because the Lennard-Jones potential reproduces the basic features that a general interatomic potential should possess: repulsive wall at short distances, a well-defined minimum, and the van der Waals r^{-6} decay of the interaction at large interatomic distances.

More general pairwise potentials can be constructed by a systematic expansion of $\Phi(r)$ using powers of the inverse distance r^{-n} . The performance of such polynomial models as a function of the maximum degree n is shown in Table 1. The improvement in atomization energies saturates around $n = 18$, reaching an accuracy of 3.0 kcal/mol. To put this number in perspective, we recall that 3 kcal/mol is below the error of the reference PBE0 atomization energies when compared with experiment.¹⁵ Moreover, the performance of the most sophisticated machine learning (ML) models in ref 16 applied to a similar data set was 3.1 kcal/mol. Therefore, it is remarkable that a simple and very efficient model based on pairwise potentials is able to capture the subtle energetic contributions required to predict atomization energies for equilibrium molecular geometries.

Seeking to better understand this finding, we plot the optimized C–C potential in Figure 2 for different values of n . The increase in the degree of the polynomial leads to the appearance of shoulders and minima related to different bond orders. In fact, these features appear at interatomic distances well-known from empirical determinations of bond orders and energies.¹⁸ We thus conclude that the increase in the degree of the polynomial enables the potential to “learn” about chemical

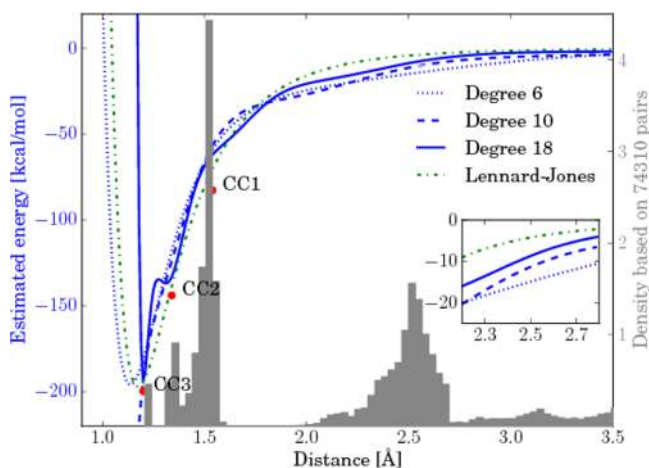


Figure 2. Polynomial potentials for C–C interaction: The normalized gray histogram refers to the distribution of C–C distances within the GDB-7 data set and is associated with the right-hand axis. The red dots represent the energies of the C–C single, double, and triple bond, as given by fits to experimental bond energies.¹⁸ In blue, polynomial two-body potentials (as trained in cross validation) are shown. The inset shows the difference between potentials for distances between 2.2 and 2.8 Å.

bonding. Similar observations as for the C–C potential are demonstrated for C–N and C–O potentials in the Supporting Information. The improvement in the predictive power of polynomial potentials does not only arise from their ability to distinguish between different bonding scenarios. The decay of these potentials with interatomic distance is rather slow, with energy contributions beyond nearest neighbors (>1.5 Å) having an essential role on the scale of the obtained error (see inset in Figure 2). We note in passing that another attractive feature of interatomic potentials is that by construction they can exactly reproduce the limit of dissociated atoms, a condition that is difficult to fulfill even in state-of-the-art *ab initio* theory. While we used polynomial potentials in this work, other choices of basis functions are certainly possible, but no significant accuracy gains are found, for example, utilizing spline-based potentials.

While the performance of pairwise potentials is already quite good, they have a few notable drawbacks. For example, their performance for out-of-equilibrium molecular geometries is strongly degraded. In order to demonstrate this, we extended the GDB-7 database by scaling all the interatomic distances in the molecules by a factor of 0.9 and 1.1. When trying to learn the atomization energies for out-of-equilibrium molecular geometries, the performance of pairwise potentials diminished by 16.7 kcal/mol compared to pure equilibrium geometries. This test demonstrates that while pairwise potentials can be successfully applied in preliminary studies of stabilities for equilibrium geometries (when these are given from some other method), more sophisticated approaches are required for nonequilibrium molecular geometries.

Evidently, collective effects beyond pairwise potentials are important for chemically accurate modeling of molecular atomization energies. To include these effects, we propose a more sophisticated ML approach, which we call Bag of Bonds (BoB). The BoB concept is inspired by text mining descriptors utilized in computer science^{19,20} (see Figure 3 and Supporting Information for a detailed description of the model). In natural language processing, the so-called bag-of-words descriptor that encodes the frequency of occurrence of words in text is used for solving classification problems.^{19,20} Here instead we propose to use interatomic (inverse) distances in the BoB descriptor for accurate predictions throughout chemical compound space. In the BoB model, first the molecular Hamiltonian is mapped to a well-defined descriptor, here a vector composed of bags, where each bag represents a particular bond type (C–C, C–N, and so on). Motivated by the Coulomb matrix concept of Rupp et al.,¹⁷ each entry in every bag is computed as $Z_i Z_j / |\mathbf{R}_i - \mathbf{R}_j|$, where Z_i and Z_j are the nuclear charges, while \mathbf{R}_i and \mathbf{R}_j are the positions of the two atoms participating in a given bond. To vectorize this information, instead of forming a matrix we simply concatenate all bags of bonds in a specified order (the order is irrelevant for the learning process), padding each bag with zeros to give the bags equal sizes across all molecules in the GDB-7 database and sorting the entries in each bag according to their magnitude. This representation is naturally invariant under molecular rotations and translations, whereas the permutational invariance is enforced by the sorting step. We note in passing that unlike the sorted Coulomb matrix¹⁷ the BoB descriptor is not able to distinguish between homometric molecules²¹ (molecules with different geometries but equal set of pairwise distances between nuclei); however, our database is devoid of such cases.

We split the full GDB-7 database into a training set of N molecules and a testing set containing the rest of the molecules

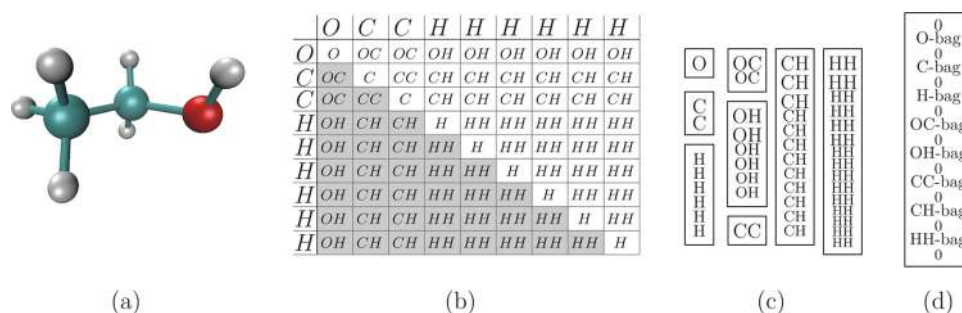


Figure 3. Schematic view of the Bag of Bonds (BoB) representation. (a) 3D structure of ethanol ($\text{CH}_3\text{CH}_2\text{OH}$) and (b) involved nuclear charges for each Coulomb matrix element. (c) Different Coulomb matrix entries that are present for ethanol are sorted into bags, and the BoB vector (d) is obtained by concatenating these bags and adding zeros to allow for dealing with other molecules with larger bags.

(cf. ref 16). The energy of a molecule with a BoB vector \mathbf{M} is written as a sum over weighted exponentials centered on every molecule I in the training set

$$\hat{E}_{\text{BoB}}(\mathbf{M}) = \sum_{I=1}^N \alpha_I \exp(-d(\mathbf{M}, \mathbf{M}_I)/\sigma) \quad (2)$$

where $d(\mathbf{M}, \mathbf{M}_I) = \sum_j \|\mathbf{M}^j - \mathbf{M}_I^j\|_p$ defines the distance (not necessarily Cartesian) between the BoB vectors \mathbf{M} and \mathbf{M}_I ($\|x\|_p$ refers to the l_p norm of x), α_I are the regression coefficients, the kernel width σ is optimized for each choice of p by 5-fold cross-validation,¹⁶ and I runs over all molecules \mathbf{M}_I in the training set of size N . The values of α_I coefficients and σ are determined by a kernel-ridge regression (KRR) procedure, as described in detail elsewhere.^{16,17} KRR is a standard robust technique in machine learning, which limits the norm of regression coefficients, α_I , thereby ensuring the transferability of the BoB model to new compounds.

To understand the physics behind the BoB model, we can decompose the BoB Laplacian kernel for a molecule \mathbf{M} as $\exp(-\sum_j \|\mathbf{M}^j - \mathbf{M}_I^j\|_p/\sigma) = \prod_j \exp(-\|\mathbf{M}^j - \mathbf{M}_I^j\|_p/\sigma)$. Taylor-series expansion of the exponential as a function of internuclear Coulomb repulsion and the subsequent product will include contributions up to infinite order in terms of bond pairs between molecules \mathbf{M} and \mathbf{M}_I . We stress that the BoB model uses implicitly the same ingredients as conventional multipolar potentials, albeit with a different, arguably more general, functional form. Simple sum over bonds and pairwise potential approaches can be constructed as lower-order expansions of the BoB model, given sufficient training data. In fact, a connection between the BoB model and pairwise potentials can be established by approximately rewriting the BoB kernel as $\sum_{l \in n_b} \prod_{j \in b_l} \exp(-\|\mathbf{M}^j - \mathbf{M}_I^j\|_p/\sigma)$, where b refers to a certain type of bond (e.g., C–C) and n_b is the length of the bag corresponding to the bond type b . We found that such partial linearization of the BoB model reduces the accuracy, reverting the performance back to the pairwise polynomial potential model. This clearly demonstrates the crucial role of collective many-bond effects accounted for by the nonlinear infinite-order nature of the kernel. We note that eq 2 only includes contributions from pairs of molecules. One could also envision more complex approaches that correlate information from three or more molecules at a time.

The flexibility in choosing the kernel metric in CCS (the function d in eq 2) allows us to investigate the locality properties of chemical space for the prediction model in terms of atomization energies. The high sensitivity of the BoB model on the employed kernel is demonstrated in Table 1, where a

more local (in terms of distance in chemical space) Gaussian kernel ($p = 2$) leads to an accuracy of 4.5 kcal/mol versus a much improved performance of 1.5 kcal/mol for a nonlocal Laplacian kernel ($p = 1$). We remark that the remarkable performance of the BoB model with the Laplacian kernel with respect to previous work^{16,17} is far from being a trivial achievement. In the context of standard quantum-chemical calculations, the improvement of accuracy from 3.1¹⁶ to 1.5 kcal/mol would imply an increase of several orders of magnitude in the computational cost; however, the cost of BoB calculations is the same as that of the previous less accurate ML methods in refs 16 and 17. Hence, the development of the BoB model takes machine learning approaches to an unprecedented level of accuracy, enabling calculations close to the “holy grail” of chemical accuracy for equilibrium molecular geometries throughout chemical compound space. We note in passing that determining equilibrium molecular geometries as an input for BoB calculations is not a difficult task, and even simple and efficient semiempirical quantum-chemical approaches yield accurate results for equilibrium molecular geometries.

To further elucidate the role of nonlocal information in chemical space in the prediction of atomization energies, we have systematically studied the dependence of the prediction accuracy on the metric norm p employed in eq 2. We find that the optimal value of p is close to unity and the predictive capability decreases significantly for $p < 0.5$ and $p > 1.5$. For larger values of p , for example, $p = 2$, the resulting model is more local and yields worse results. For kernel-based models, it is possible to calculate the contribution to the predicted value for each compound in the training set. Adding up all contributions from compounds close to the compound in question, we obtain a “local estimate” of the predicted value. Figure 4 illustrates how this local estimate of the atomization energy converges toward the predicted value with randomly selected and growing molecular neighborhoods in the case of ethanol molecule for Gaussian and Laplacian kernels. Clearly, the Laplacian kernel is able to optimally utilize nonlocal information in CCS. This is further demonstrated by analyzing the optimized kernel width σ in eq 2 corresponding to the Gaussian and Laplacian kernels. The value of σ fluctuates widely for the Gaussian kernel for different training set sizes in Figure 4, as does the standard deviation when training on independently drawn training sets. The corresponding fluctuations are smaller for the Laplacian kernel, and σ reaches its converged value after $N = 500$. Similar results as for ethanol are found for the other molecules in the GDB-7 database. The issue of (non)locality in the accurate prediction of molecular

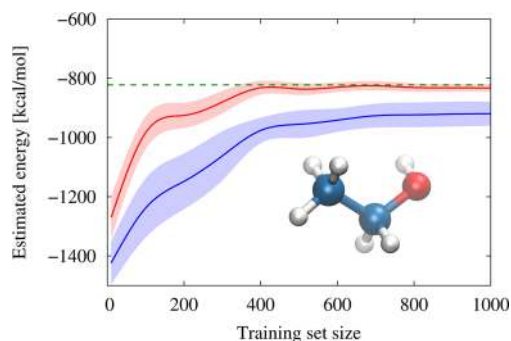


Figure 4. Estimated atomization energy of the ethanol molecule ($\text{C}_2\text{H}_5\text{OH}$) as predicted by the BoB model using Gaussian (blue line) and Laplacian (red line) kernels. The PBE0 reference energy is indicated by the dashed green line. For a given training set size, the estimation is an average of predictions from 10 optimized models, each employing independently sampled training molecules (excluding ethanol) from the GDB-7 database. The envelope encloses the standard deviation of the estimate from 10 independent runs.

properties leads to the question of whether it is possible to identify a minimal set of molecular structural fragments that would be sufficient to preserve the good accuracy of the BoB model. Such finding would allow us to extend the applicability of the BoB model to much larger molecules, and this will be a subject of our future work.

In contrast with pairwise potentials, the good performance of the BoB approach also extends to nonequilibrium molecular geometries. For the extended GDB-7 database with stretched and compressed geometries previously described, the prediction error of BoB increases by only 0.8 kcal/mol. This is a direct reflection of the ability of the BoB approach to correctly capture the intricate collective interactions between many bonds within organic molecules.

Another advantage of the BoB model over pairwise potentials is its better transferability and smooth prediction improvement with the number of training samples, as shown in Figure 5.

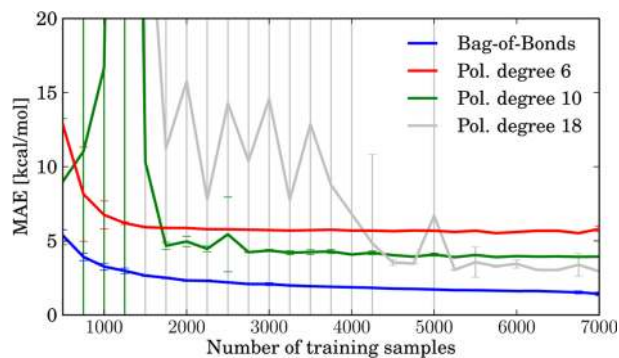


Figure 5. Mean absolute error (MAE in kcal/mol) for BoB and polynomial models: Training sets from $N = 500$ to 7000 data points were sampled identically for the different methods. The polynomial models of degree 10 and 18 exhibit high variances due to the random stratification, which for small N leads to nonrobust fits.

Already when using just 1000 random molecules out of GDB-7 for training the BoB model demonstrates prediction accuracy comparable to the best optimized polynomial potential with degree 18, which requires more than 5000 training samples to achieve the same level of accuracy. At a first glance, this is surprising considering that the polynomial potential contains

less adjustable parameters. However, Figure 5 demonstrates that BoB represents a more robust machine learning model with proper regularization and that further improvement in accuracy is possible by simply enlarging the molecular database. This demonstrates the great promise of the BoB approach for further exploration and understanding of CCS.

The applicability and accuracy of the BoB model also extends for predicting properties other than energies, including polarizability and highest and lowest molecular orbital energies (HOMO, LUMO), all computed at the DFT-PBE0 level of theory. BoB error distributions for out-of-sample predictions are shown in Figure 6. For models trained on $N = 1000$ GDB-7

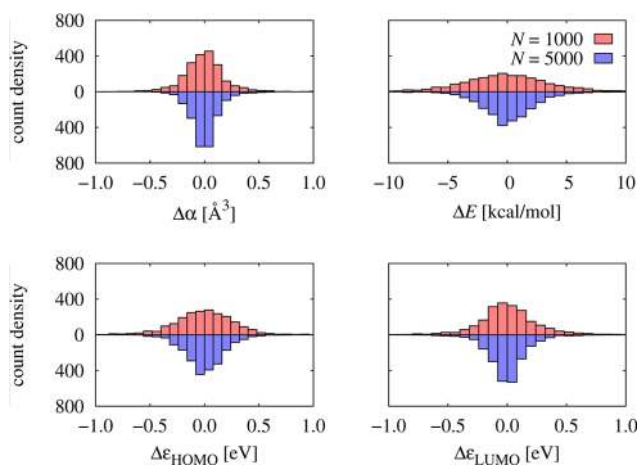


Figure 6. Error distribution of BoB predicted electronic properties polarizability (α), atomization energy (E), and HOMO and LUMO eigenvalues (ϵ) for 2165 randomly drawn out-of-sample molecules from GDB-7 for training set sizes of $N = 1000$ and 5000, respectively.

molecules with property data taken from ref 22, the resulting MAEs are 0.15 \AA^3 , 0.21 eV, and 0.19 eV for polarizability (mean of 11.11 \AA^3), HOMO (mean of -7.02 eV), and LUMO (mean of -0.52 eV), respectively. For the $N = 5000$ BoB model, these respective errors reduce to 0.09 \AA^3 , 0.14 eV, and 0.12 eV. We remark that the BoB model once again performs as well as or better than the more complex ML models in the literature.²²

The final question we would like to address is the feasibility of utilizing the BoB model in the context of high throughput calculations on molecular systems. This requires the assessment of the BoB model on a much larger data set of molecules. To demonstrate that the power and robustness of our method extends beyond GDB-7, we employed the 134k data set of quantum-chemical calculations (containing 133 885 molecules), recently presented in ref 23. Similar to the case of GDB-7 data set, we obtain an accuracy of 2.0 kcal/mol for atomization energies in the 134k data set when training the BoB model on 30% of the molecules.

In summary, we have devised and applied a systematic hierarchy of efficient models to estimate atomization energies and different electronic properties for a representative set of organic molecules. The developed BoB model is quite successful for nonequilibrium geometries, hinting that it could also be extended to study vibrational properties of molecules. In addition, the BoB model is demonstrated to be sufficiently robust as a tool in the context of high-throughput calculations throughout a representative subset of the chemical compound space.

■ ASSOCIATED CONTENT

● Supporting Information

Detailed description of the Bag of Bonds (BoB) model, kernel parameters, and pairwise potentials. The Supporting Information is available free of charge on the ACS Publications website at DOI: 10.1021/acs.jpclett.5b00831.

■ AUTHOR INFORMATION

Corresponding Authors

*K.-R.M.: E-mail: klaus-robert.mueller@tu-berlin.de.

*A.T.: E-mail: tkatchenko@fhi-berlin.mpg.de.

Notes

The authors declare no competing financial interest.

■ ACKNOWLEDGMENTS

We thank Dr. Matthias Rupp for inspiring discussions. This work is supported by the European Research Council (ERC-StG VDW-CMAT), DFG Grant No. MU 987/20, Natural Sciences and Engineering Research Council of Canada, by the BK21 program of NRF, the Einstein Foundation, and the Swiss National Science Foundation (Grant No. PP00P2_138932). This work used resources of the Argonne Leadership Computing Facility at Argonne National Laboratory, which is supported by the Office of Science of the U.S. DOE under Contract No. DE-AC02-06CH11357.

■ REFERENCES

- (1) Kirkpatrick, P.; Ellis, C. Chemical Space. *Nature* **2004**, *432*, 823.
- (2) Schneider, G. Virtual Screening: An Endless Staircase? *Nat. Rev.* **2010**, *9*, 273.
- (3) Todeschini, R.; Consonni, V. *Handbook of Molecular Descriptors*; Wiley-VCH: Weinheim, Germany, 2009.
- (4) Manzhos, S.; Carrington, T. Using Neural Networks to Represent Potential Surfaces as Sums of Products. *J. Chem. Phys.* **2006**, *125*, 194105.
- (5) Behler, J.; Parrinello, M. Generalized Neural-Network Representation of High-Dimensional Potential-Energy Surfaces. *Phys. Rev. Lett.* **2007**, *98*, 146401.
- (6) Behler, J. Atom-Centered Symmetry Functions for Constructing High-Dimensional Neural Networks Potentials. *J. Chem. Phys.* **2011**, *134*, 074106.
- (7) Bartók, A. P.; Payne, M. C.; Kondor, R.; Csányi, G. Gaussian Approximation Potentials: The Accuracy of Quantum Mechanics, without the Electrons. *Phys. Rev. Lett.* **2010**, *104*, 136403.
- (8) Fletcher, T. L.; Davie, S. J.; Popelier, P. L. Prediction of Intramolecular Polarization of Aromatic Amino Acids using Kriging Machine Learning. *J. Chem. Theory Comput.* **2014**, *10*, 3708–3719.
- (9) Fink, T.; Bruggesser, H.; Reymond, J.-L. Virtual Exploration of the Small-Molecule Chemical Universe Below 160 Da. *Angew. Chem., Int. Ed.* **2005**, *44*, 1504.
- (10) Fink, T.; Reymond, J.-L. Virtual Exploration of the Chemical Universe up to 11 Atoms of C, N, O, F: Assembly of 26.4 Million Structures (110.9 Million Stereoisomers) and Analysis for New Ring Systems, Stereochemistry, Physicochemical Properties, Compound Classes, and Drug Discovery. *J. Chem. Inf. Model.* **2007**, *47*, 342.
- (11) Guha, R.; Howard, M. T.; Hutchison, G. R.; Murray-Rust, P.; Rzepa, H.; Steinbeck, C.; Wegner, J.; Willighagen, E. L. The Blue Obelisk - Interoperability in Chemical Informatics. *J. Chem. Inf. Model.* **2006**, *46*, 991.
- (12) Perdew, J. P.; Burke, K.; Ernzerhof, M. Generalized Gradient Approximation Made Simple. *Phys. Rev. Lett.* **1996**, *77*, 3865.
- (13) Blum, V.; Gehrke, R.; Hanke, F.; Havu, P.; Havu, V.; Ren, X.; Reuter, K.; Scheffler, M. Ab Initio Molecular Simulations with Numeric Atom-Centered Orbitals. *Chem. Phys. Commun.* **2009**, *180*, 2175.
- (14) Perdew, J. P.; Ernzerhof, M.; Burke, K. Rationale for Mixing Exact Exchange with Density Functional Approximations. *J. Chem. Phys.* **1996**, *105*, 9982.
- (15) Lynch, B. J.; Truhlar, D. G. Robust and Affordable Multicoefficient Methods for Thermochemistry and Thermochemical. *J. Phys. Chem. A* **2003**, *107*, 3898.
- (16) Hansen, K.; Montavon, G.; Biegler, F.; Fazli, S.; Rupp, M.; Scheffler, M.; von Lilienfeld, O. A.; Tkatchenko, A.; Müller, K.-R. Assessment and Validation of Machine Learning Methods for Predicting Molecular Atomization Energies. *J. Chem. Theory Comput.* **2013**, *9*, 3404.
- (17) Rupp, M.; Tkatchenko, A.; Müller, K.-R.; von Lilienfeld, O. A. Fast and Accurate Modeling of Molecular Atomization Energies with Machine Learning. *Phys. Rev. Lett.* **2012**, *108*, 058301.
- (18) Benson, S. W., III. Bond Energies. *J. Chem. Educ.* **1965**, *42*, 502.
- (19) Forman, G. An Extensive Empirical Study of Feature Selection Metrics for Text Classification. *J. Mach. Learn. Res.* **2003**, *3*, 1289.
- (20) Joachims, T. Text Categorization with Support Vector Machines: Learning with Many Relevant Features. *ECML '98 Proc. 10th Eur. Conf. Mach. Learn.* **1998**, 137–142.
- (21) Patterson, A. L. Homometric Structures. *Nature* **1939**, *143*, 939.
- (22) Montavon, G.; Rupp, M.; Gobre, V.; Vazquez-Mayagoitia, A.; Hansen, K.; Tkatchenko, A.; Müller, K.-R.; von Lilienfeld, O. A. Machine Learning of Molecular Electronic Properties in Chemical Compound Space. *New J. Phys.* **2013**, *15*, 095003.
- (23) Ramakrishnan, R.; Dral, P. O.; Rupp, M.; von Lilienfeld, O. A. Quantum Chemistry Structures and Properties of 134 Kilo Molecules. *Sci. Data* **2014**, *1*, 140022.